

Digital Image Analysis of Sheet Metal Testing and Forming

Szabolcs Szalai¹, Imre Czinege²

¹ Széchenyi István University, Győr, Hungary. szalai@sze.hu

² Széchenyi István University, Győr, Hungary. czinege@sze.hu

Abstract – Digital image analysing methods are widely used for evaluating local deformations in sheet metal tests and forming processes. The paper is focusing on tensile tests of uniform and non-uniform width flat specimens made of aluminum alloys, which are suitable for demonstrating Lüders strain, Portevin-Le Chatelier (PLC) effect and for determination of Forming Limit Curve. Tests were carried out using GOM-ARAMIS® digital image analysis hardware and software. Observation of local deformations during tensile tests showed that initiation and evolution of local strains depend on the position of specimens related to rolling direction of sheet. Using non-uniform width specimens the local deformations are concentrated on the smallest cross-section in the final stage of tensile test. The measured major and minor strains give points of FLC.

I. INTRODUCTION

Digital image analysing methods are widely used for evaluating local deformations in sheet metal tests and forming processes. During tensile tests mainly Lüders effect, phenomena of serrated yielding and diffuse or local necking can be observed. Sheet metal forming tests – for example Erichsen- and dome-test, determination of forming limit curve (FLC) – are often analysed also with digital optical methods.

Measurement of local deformations can be carried out by different patterns applied on the surface. These patterns might be either regular (circle grid analysis, CGA) or random, like speckles on a painted base color which form a stochastic intensity pattern on the object surface. The basic method used for evaluation of patterns is Digital Image Correlation (often referred to as “DIC”) which measures deformation on an object’s surface.

The metallographic phenomena studied in this paper are Lüders-bands and serrated yielding during tensile test using test specimens of different shaped (with uniform and non-uniform cross-section). The theoretical background of these subjects are the followings.

A. Principle and Application of Digital Image Correlation

The approach for determining surface deformation

using digital image correlation technique has started from the 1980s, later the solutions have been improved by many researchers and companies [1]. Nowadays, several applications of this method to various problems can be found, such as in studies of material testing, metal forming, wood and polymer testing, stress analysis or in large scale measurements of aerospace, automotive, marine, railway and civil engineering components. Two basic solutions are available, the 2D measurement for plane specimens and 3D systems for spatial components. In both cases displacements are directly detected from digital images of the surface. The 2D plane surface can be observed by one digital camera while for spatial (3D) measurements 2 or 4 cameras are used. During tests the images on the surface of the object are recorded, digitized and stored in a computer. Usual test speed is 10-50 frame/sec depending on the process. These images are compared to detect displacements by searching matched points from one image to another. From these displacements the principal strains can be evaluated.

Many companies offer ready-made hardware and software solutions for material testing applications. For example, Instron® DIC Replay Software [2] is a self-contained 2D package which creates pictures that can be used to visualize strain and displacement over the full two dimensional surface of the tensile test specimen. The GOM-ARAMIS® measuring system [3] is using random pattern (speckles) on the surface to determine material properties. These are for example Young’s modulus, r - and n -value during tensile tests, forming limit curve determination by Nakajima test. The other GOM solution, ARGUS formability system is the automated version of circle grid analysis which can be used for measuring of local deformations in sheet metal forming. In this case a regular circle grid is applied in a plane surface, then deformation process is carried out and finally local strains are calculated. The VIALUX AutoGrid® in-process device [4] applies CGA method and measures the specimen while it is being test loaded, so the system supports the recording of deformations and strains during a forming process. For the measurement of forming limit curves (FLC) four cameras observe the specimen from different perspective views, after deformation the software automatically evaluates the FLC. Many authors have been analysed the effect of grid

size on the results, for example [5] showed that change in mesh size of 0,5, 1 and 2 mm influences the form of FLC. Detailed survey can be found in [6] for specimens with speckled pattern, where the authors compared the results of DIC method with strain gage measurements in case of tensile and compression tests.

B. Introduction to Lüders Effect and Serrated Yielding

Al-based alloys are extensively used in the automotive industry due to their low density, high strength, and good formability [7,8]. These properties are advantageous from a manufacturing point of view. However, the heterogeneous deformation of Al-based alloys (even 5xxx series) subjected to a high strain gradient represents a major drawback of these materials. This phenomenon leads to undesirable visible traces on the surface of the final products. The induced heterogeneous deformation can be classified into two general categories: the Lüders effect and the Portevin-Le Chatelier (PLC) effect [9,10]. The visible presence of Lüders effect is that the stress-strain curves show a plateau just after the end of elastic deformation. This is called the yield-point phenomenon, and the elongation which occurs at constant stress is called the yield-point elongation or Lüders strain. The deformation throughout the Lüders elongation is heterogeneous. With the occurrence of Lüders elongation, a Lüders band can be visible passing along from one end of the sample to the other. The Lüders effect results from the dislocation pinning/unpinning effect arising from Cottrell atmosphere constraints and the collective or self-organized dislocation multiplication and motion. Serrated yielding occurs on the part of stress-strain curves after the Lüders elongation because of the PLC effect. This is typically attributed to dynamic interactions between mobile dislocations and diffusing solutes (i.e., dynamic strain ageing, DSA). In AlMg alloys the serration intensity increases with an increase in Mg content. The Lüders effect and serrated yielding can be associated with tensile stress-strain diagram, which can be seen on Fig. 1.

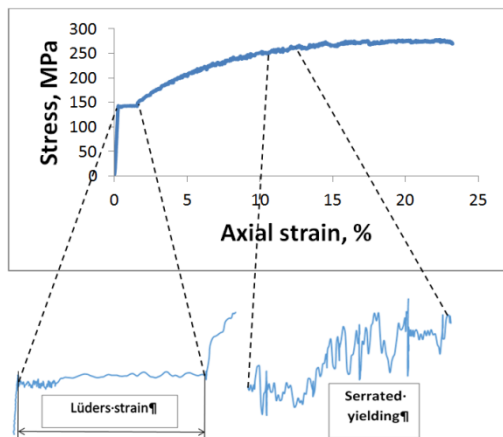


Fig. 1. Illustration of Lüders strain and serrated yielding

Both phenomena can be visualised on the surface of tensile test specimens by digital image correlation methods [9-13]. The mentioned papers are focusing on AlMg alloys and they are discussing both Lüders effect and serrated yielding. From the time-dependent digital images the velocity and evolution of Lüders bands can be evaluated. Similarly the serrated yielding is identified and characterised. The other possibility for characterising serrated yielding can be connected to tensile stress-strain diagram. The shape, magnitude and frequency of serrations have been analysed in the literature in details [14-18].

II. EXPERIMENTS

The materials for this investigation are AA3014 and AA5182 aluminum alloys. Their chemical composition is listed in Table 1.

Table 1. Chemical composition of alloys

	Si	Fe	Cu	Mn	Mg	Zn
AA3004	0,269	0,482	0,153	0,796	1,200	0,044
AA5182	0,127	0,255	0,053	0,259	4,930	0,044

Samples for tensile testing were cut along the rolling direction (RD, 0°), transverse direction (TD, 90°) and diagonal direction (DD, 45°). The tests were carried out using uniform and non-uniform width specimens. The measuring area of standard uniform width specimens was 80x20 mm. Fig. 2. shows the dimensions of a non-uniform width specimen, where appropriate radii from 5 to 40 mm were applied to establish different major/minor strain ratios.

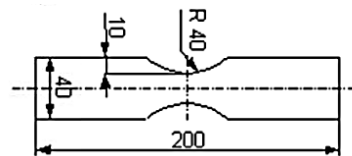


Fig. 2. Shape of test specimen of non-uniform width

Tensile test results for AA 3004 and AA5182 alloys can be seen in Table 2. Strength and formability properties do not show significant anisotropy of sheets except plastic strain ratio (r) in case of AA5182 sheet.

Table 2. Mechanical properties of tested alloys

Alloy	R _{p0.2} , MPa	R _m , MPa	A _g , %	A ₈₀ , %	n	r	
AA3004	0°	73	172	7,77	9,41	0,37	0,68
	45°	71	160	7,49	9,12	0,33	0,72
	90°	76	158	6,15	8,65	0,33	0,71
AA5182	0°	119	236	10,33	10,53	0,378	0,61
	45°	123	259	16,26	16,53	0,341	1,06
	90°	124	245	13,40	13,60	0,333	0,74

The novelty of tests was that the thickness of samples were 0,22 and 0,3 mm and the average grain size was

ranging between 25-35 μm , roughly one tenth of the thickness. This is why the grain size effect influences the surface roughness and the formation of bands. Nine samples were prepared for each material using 3-3 cut in different directions to rolling axle (RD, DD, TD). Tensile testing was carried out on a 2 kN capacity Instron® machine and GOM-ARAMIS software controlled the entire process, the load versus elongation values were stored automatically and at the meantime digital images were recorded also by the system. Nominal strain rate $2 \cdot 10^{-3} \text{ s}^{-1}$ was employed for each material.

Standard GOM-ARAMIS® technique was used for analysing the local deformations of samples during tensile test. The frame rate of sampling was 4/sec, considering of the applied strain rate it means that $\Delta\epsilon$ between samples was 0,03% strain.

III. EXPERIMENTAL RESULTS

A. Local deformations of tensile test specimens

About 400 frames were recorded during tensile tests carried out with uniform-width specimens. The automatic evaluation of GOM-ARAMIS software contains the photo of deformed specimen with speckled pattern, the distribution of strains and the position of measurement in the tensile test diagram. The most interesting results of AA3004 sheet can be seen in the followings. Fig. 3. shows the evolution of local strains at the end of elastic region in both directions to rolling axle. Although the overall strain of specimens is roughly the same ($\epsilon_{pl}=0,3...0,5\%$), significant differences can be observed in different directions.

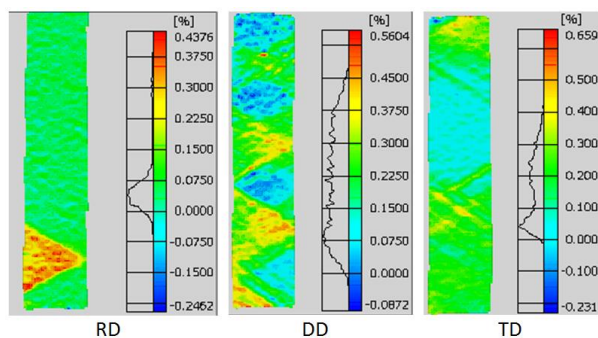


Fig. 3. Evolution of local strains (AA3004)

In the region of plastic deformation (see Fig. 1.) the intensive and less intensive strain regions are located along the specimen. Fig. 4. shows the evolution of deformation in three strain-steps from 3,12% to 3,24%. It can be concluded that deformation bands are expanding as the average strain increases, but the local deformation areas are inhomogeneous. Fig. 5. shows that the direction of bands to rolling direction is varying according to the position of samples in the sheet. The angle of bands to longitudinal axis is 55...59°, which is similar to angles

published in the literature [10, 11]. In case of AA3004 samples the orientation is symmetrically different in rolling and transverse direction while in diagonal direction (45°) the slope of bands might be either positive or negative (Fig.5.a.). On the other hand the AA5182 samples show mixed orientation in both directions as Fig.5.b illustrates this.

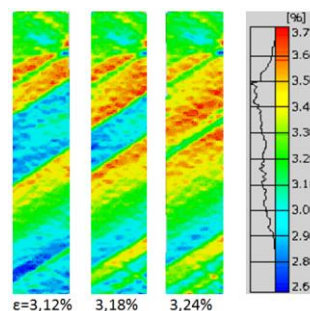


Fig. 4. Evolution of deformation bands (AA3004)

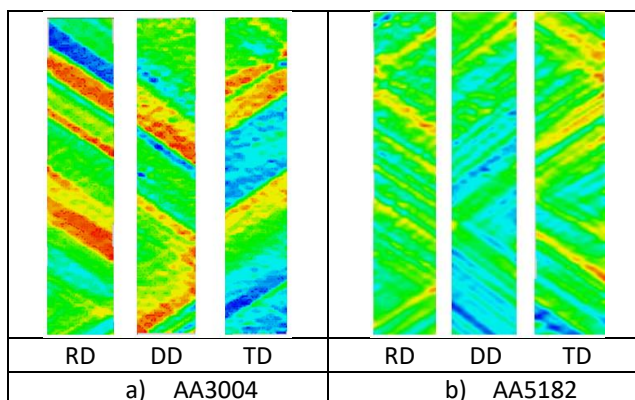


Fig. 5. Direction of deformation bands

B. Evaluation of plastic strain ratio

GOM-ARAMIS software allows to measure both longitudinal and transversal strain. From these strains the plastic strain ratio “r” can be evaluated, which characterizes the resistance of sheet against thinning.

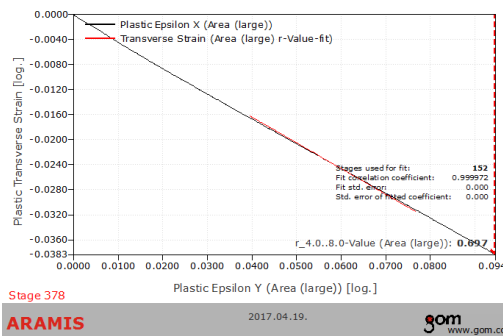


Fig. 6. Plot of longitudinal and transverse strain

Technically the R value can be calculated from the slope of longitudinal and transverse strain line. Fig. 6. shows the plot of strain function and the value of r, which is given as 0,697 in RD. This is realistic value for AA5182 sheet, although it slightly differs from the value calculated by conventional tensile test (see Table 2.). It should be noted that if longitudinal and transverse strain is measured with video extensometer using two dedicated points in both directions, then the line of two strains is not so smooth and linear as in case of DIC measurement plot. This shows an additive advantage of this technique against conventional tensile test measurements.

C. Local deformations of non-uniform samples

Fig. 2. shows the dimensions of a non-uniform width specimen. These specimens are suitable for determination of the left side of Forming Limit Curve (FLC), which has a high significance in metal forming.

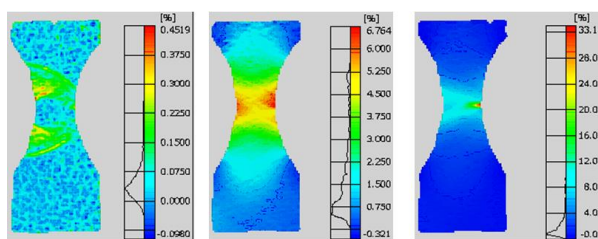


Fig. 5. Deformation phases of rounded specimen

Because of the non-uniform width the deformation of this specimen is different from those discussed former. The left side photo of Fig. 5. illustrates the beginning of deformation, the localization of strain can be observed in the middle and finally on the right side the last frame is visible before fracture. The major and minor strain can be evaluated automatically using GOM-ARAMIS software, the measured minor strain is -0,010 while major strain is +0,087. From the results of more similar specimens of different radii the left side of FLC can be plotted. The right side of FLC can be obtained from Nakazima or Marciniak test using also DIC technique for evaluating local deformations.

IV. SUMMARY

Tests of AA3004 and AA5182 alloys have proved that digital image correlation technique is suitable for determining local strains during tensile test of different specimens. The alloys show the phenomena of Lüders strain and PLC effect which can be characterized by slip bands on the surface of sheets. Comparison of specimens in different angles related to rolling direction showed different slip band patterns. Additional advantage of DIC technique is that overall longitudinal and transversal deformation of tensile test specimens can measure better than in case of conventional tensile tests and gives exact information on plastic strain ratio.

V. ACKNOWLEDGEMENTS

This research has been supported by the „Highly industrialised region on the west part of Hungary with limited R&D capacity: Research and development programs related to strengthening the strategic future oriented industries manufacturing technologies and products of regional competences carried out in comprehensive collaboration” program of the National Research, Development and Innovation Fund (NKFI), Hungary, Grant. No. VKSZ_12-1-2013-0038.

REFERENCES

- [1] M. A. Sutton: Image-based Measurements in Solid Mechanics: A Brief History, Static and Dynamic Application Examples and Recent Developments. BSSM 50th Anniversary, 2014.
- [2] <http://www.instron.us/en-us/products/materials-testing-software/dic-replay>
- [3] <http://www.gom.com/metrology-systems/aramis.html>
- [4] <https://www.vialux.de/en/in-process.html>
- [5] M. Bhargava, A. Tewari, S. Mishra: Strain path diagram simulation of AA 5182 Aluminum alloy. Procedia Engineering 64 (2013) 1252 – 1258
- [6] Po-Chih Hung and A. S. Voloshin: In-plane Strain Measurement by Digital Image Correlation. J. of the Braz. Soc. of Mech. Sci. & Eng. Copyright Ó 2003 by ABCM July-September 2003, Vol. XXV, No. 3 / 215
- [7] Automotive Megatrends USA: Aluminum – Part of the Solution. http://drivealuminum.wpengine.com/wp-content/uploads/2016/06/AutoMegatrends_4MAR.pdf
- [8] JIM DICKSON: DRIVING INNOVATION WITH AUTOMOTIVE ALUMINUM. <http://drivealuminum.wpengine.com/wp-content/uploads/2016/06/ATG-CCIF-Presentation-Short-FINAL.pdf>
- [9] Wen, Wei: A study of serrated yielding, texture and formability of 5xxx series aluminum alloys. ProQuest Dissertations And Theses; Thesis (Ph.D.)-University of Kentucky, 2004.; Publication Number: AAI3158271; ISBN: 9780496906666; Source: Dissertation Abstracts International, Volume: 65-12, Section: B, page: 6605.; 218 p.
- [10] Yu-Long Cai, Su-Li Yang, Shi-Hua Fu and Qing-Chuan Zhang: The Influence of Specimen Thickness on the Lüders Effect of a 5456 Al-Based Alloy: Experimental Observations. Chinese Academy of Science Key Laboratory of Mechanical Behaviour and Design of Materials, University of Science and Technology of China, Hefei 230027, China
- [11] Y.L.Cai, S.L.Yang, Y.H.Wang, S.H.Fu, Q.C.Zhang: Characterization of the deformation behaviours associated with the serrated flow of a 5456 Al-based

- alloy using two orthogonal digital image correlation systems. *Materials Science & Engineering A* 664 (2016) 155–164.
- [12] Wei Wen, Yumin Zhao, J.G. Morris: The effect of Mg precipitation on the mechanical properties of 5xxx aluminum alloys. *Materials Science and Engineering A* 392 (2005) 136–144
- [13] Wei Tong, Nian Zhang: On Serrated Plastic Flow in an AA5052-H32 Sheet. *Transactions of the ASME*, Vol. 129, April 2007. 332-341
- [14] E. Isaac Samuel, J. Christopher, G. Sainath, B.K. Choudhary: Unified description of tensile work hardening behaviour of P92 steel. *Materials Science & Engineering A* 652 (2016) 92–98
- [15] W. Kilpatrick, D. Brown, R.J. McMurray, A.G. Leacock: The effect of serrated yielding on the determination of r-values in aluminium alloys and yield locus calibration. *Materials Science and Engineering A* 527 (2010) 7557–7564
- [16] S.P. Joshi & C. Eberl & B. Cao & K.T. Ramesh & K.J. Hemker: On the Occurrence of Portevin–Le Châtelier Instabilities in Ultrafine-Grained 5083 Aluminum Alloys. *Experimental Mechanics*, 2009, DOI 10.1007/s11340-008-9208-3
- [17] G. Saad, S.A. Fayek, A. Fawzy, H.N. Soliman, E. Nassr: Serrated flow and work hardening characteristics of Al-5356 alloy. *Journal of Alloys and Compounds* 502 (2010) 139–146
- [18] Matthew Wagenhofer, MarjorieAnn Erickson-Natishan, Ronald W. Armstrong and Frank J. Zerilli: INFLUENCES OF STRAIN RATE AND GRAIN SIZE ON YIELD AND SERRATED FLOW IN COMMERCIAL Al-Mg ALLOY 5086. *Scripta Materialia*, Vol. 41, No. 11, pp. 1177–1184, 1999